

Synthesis, characterization and use of benzothioxanthene imide based dimers

José María Andrés Castán, Clément Dalinot, Sergey Dayneko, Laura Abad Galan, Pablo Simón Marqués, Olivier Alévêque, Magali Allain, Olivier Maury, Ludovic Favereau, Philippe Blanchard, et al.

▶ **To cite this version:**

José María Andrés Castán, Clément Dalinot, Sergey Dayneko, Laura Abad Galan, Pablo Simón Marqués, et al.. Synthesis, characterization and use of benzothioxanthene imide based dimers. Chemical Communications, 2020, 56 (70), pp.10131-10134. 10.1039/d0cc04556j . hal-02930352

HAL Id: hal-02930352
https://hal.science/hal-02930352

Submitted on 19 Nov 2020

HAL is a multi-disciplinary open access archive for the deposit and dissemination of scientific research documents, whether they are published or not. The documents may come from teaching and research institutions in France or abroad, or from public or private research centers.

L'archive ouverte pluridisciplinaire **HAL**, est destinée au dépôt et à la diffusion de documents scientifiques de niveau recherche, publiés ou non, émanant des établissements d'enseignement et de recherche français ou étrangers, des laboratoires publics ou privés.

COMMUNICATION

Synthesis, characterization and use of benzothioxanthene imide based dimers

Received 00th January 20xx,
Accepted 00th January 20xx

DOI: 10.1039/x0xx00000x

José María Andrés Castán,[a]† Clément Dalinot,[a]† Sergey Dayneko,[b] Laura Abad Galan,[c] Pablo Simón Marqués,[a] Olivier Alévêque,[a] Magali Allain,[a] Olivier Maury,[c] Ludovic Favereau,[d] Philippe Blanchard,[a] Gregory C. Welch, *[b] and Clément Cabanetos*[a]

The synthesis of benzothioxanthene imide based dimers is reported herein. Subtle chemical modifications were carried out and their impact on the optical and electrochemical properties investigated for a better structure-property relationships analysis. Icing on the cake, these new structures were used as light emitting materials for the fabrication and demonstration of the first BTXI-based OLEDs.

Over the years, imide containing rylenes have demonstrated their potential as strong candidates for a variety of organic electronic applications due to their excellent thermal, chemical and photochemical stabilities, as well as intriguing electronic and redox properties.[1] Perylene and naphthalene diimides can be clearly identified as the beacons of this molecular family in terms of reported studies, chemical modifications and target applications (Figure 1).[2]

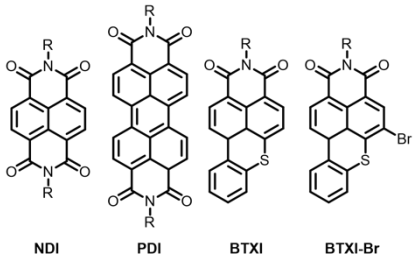
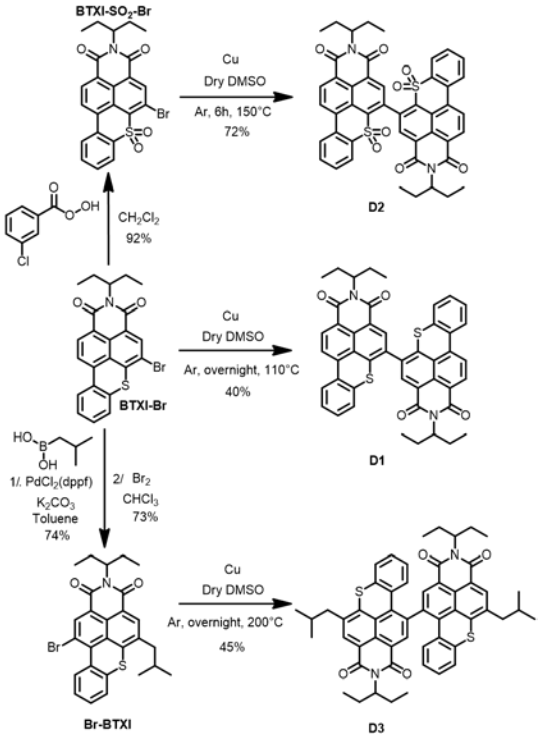


Figure 1. *Structure of NDI, PDI, BTXI and BTXI-Br.*

Motivated by the exploration and functionalization of original chemical structures, we have recently focused our attention on an overlooked and inexpensive vat dye, the benzothioxanthene imide (**BTXI**). Never used for organic electronic purposes and exclusively functionalized on the nitrogen atom of the imide group, we have reported the selective and efficient mono-bromination of its rylene core, affording the **BTXI-Br** (Figure 1),[3, 4] and have opened the door to the design of new and original molecular architectures that have been successfully evaluated as active materials in organic photovoltaic (OPV) devices.[5, 6] Consequently, to further explore the potential of this dye, we report herein the synthesis and use of three dimers to prepare the first **BTXI**-based organic light-emitting diodes (OLEDs).

As depicted in scheme 1, target molecules stemmed from the common **BTXI-Br** derivative. The later was indeed either sulfonated (**BTXI-SO_2-Br**) or engaged in a Suzuki-Miyaura cross-coupling reaction in order to be subsequently and efficiently mono-brominated at the bay position (**Br-BTXI**).



Scheme 1. *Synthetic route to **D1**, **D2** and **D3**.*

[a] *CNRS UMR 6200, MOLTECH-Anjou, University of Angers, 2 Bd Lavoisier, 49045 Angers, France*
[b] *Department of Chemistry, University of Calgary, 2500 University Drive N.W., Calgary, Alberta T2N 1N4, Canada*
[c] *Univ Lyon, ENS de Lyon, CNRS UMR 5182, Université Claude Bernard Lyon 1, F-69342 Lyon, France. Univ Rennes, CNRS, ISCR – UMR 6226, ScanMAT – UMS 2001, F-35000 Rennes, France.*
† *both authors equally contributed to this work*
Electronic Supplementary Information (ESI) available: [details of any supplementary information available should be included here]. See DOI: 10.1039/x0xx00000x

Please do not adjust margins

Table 1. *Optical and electrochemical data recorded for* ***D1, D2*** *and* ***D3.*** *[a] in solution and [b] on powders.*

Dimer	λ_{abs} (nm)	ε (M^{-1} cm^{-1})	λ_{em} (nm)	$\Phi_f{}^a$	$\lambda_{em}{}^b$ (nm)	$\Phi_f{}^b$	E_{pa} ($V_{Fc+/Fc}$)	E_{pc} ($V_{Fc+/Fc}$)	E_{HOMO} (eV)	E_{LUMO} (eV)	ΔE_{elec} (eV)
BTXI	455	22000	502	0.99	579	0.02	0.94	-1.82	-5.63	-3.10	2.53
D1	455	51000	509	0.19	534	0.06	1.00	-1.74	-5.64	-3.16	2.48
D2	384	37000	450	0.29	460	0.14	1.47	-1.18	-6.07	-3.73	2.35
D3	473	31000	530	0.34	580	0.18	0.86	-1.70	-5.54	-3.21	2.32

Finally, dimers **D1**, **D2** and **D3** were prepared from the corresponding bromo derivatives, namely **BTXI-Br**, **BTXI-SO_2-Br** and **Br-BTXI** respectively, under copper-catalyzed Ullmann reaction conditions.[7] In parallel, pallado-catalyzed cross coupling conditions have been applied, in a further attempt to improve the synthetic yields, particularly for **D1** and **D3**, but were not found to be that much convincing (Scheme S1).

Single crystals of all the dimers were prepared by slow evaporation techniques. In addition to confirming the structures, the latter highlighted, as expected, large dihedral angles between the constituting **BTXI** units of *ca.* 75.9, 75.6 and 60.2 for **D1**, **D2** and **D3** respectively (Figure 2). Such important twists might contribute to the good solubility of the derivatives and should profoundly modify the self-assemble properties compared to those of the **BTXI** monomer, and consequently tune the solid-state luminescence (*vide supra*). Comparison of crystal packing indicates that (i) **BTXI** forms a very regular head-to-tail stacking with strong cofacial π-interactions (d= 3.675 and 3.816 Å, Figure S20); (ii) **D1** and **D2** crystallized as dimers with strong and moderate intermolecular π-interactions respectively (Figures S21 and S22); and **D3** forms more complex hexameric toroidal structure with circular slipped π-interactions between two vicinal molecules (Figures S23-S25).

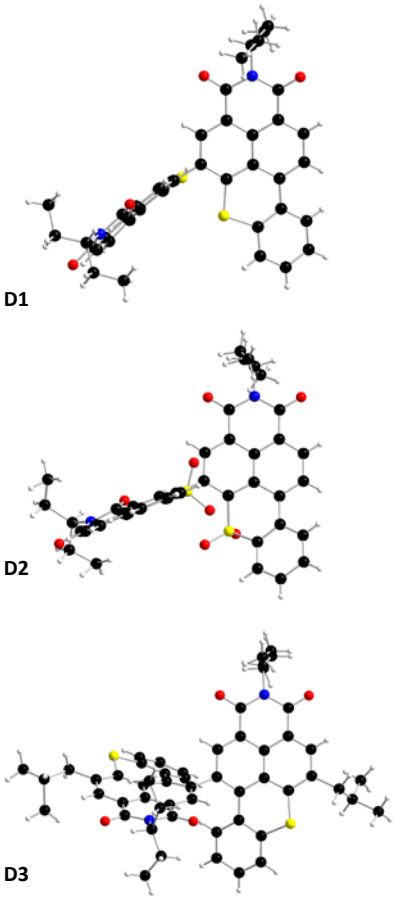


Figure 2. *X-ray structures of* ***D1, D2*** *and* ***D3****.*

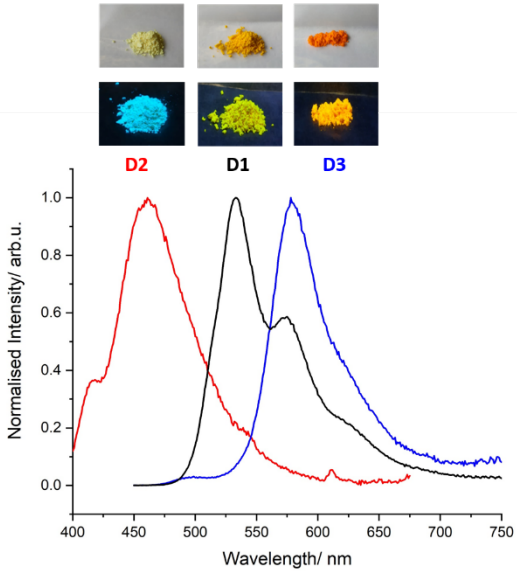


Figure 3*. (a) Photograph of powders of* ***D1, D2*** *and* ***D3*** *under white light (top) and 254 nm (bottom) and b) their respective emission spectra.*

In parallel, the photophysical properties have been investigated in both diluted dichloromethane solution and in the solid state. Results are gathered in the Table 1. In solution, it appears that oxidation into sulfones (**D2**) induces a significant blue shift (of *ca*. 50 nm) of the long-wavelength absorption band (π-π* transitions) initially centered around 450 nm (**D1, D3**) (Figure S16 and S28), in agreement with the previously reported **BTXI-SO_2** derivative.[8] A similar effect is also observed in the emission. Importantly, compared to **BTXI**,[8] the dimerization results in a significant decrease of the luminescence quantum yield in solution (Table 1). This effect is explained by a more favoured intersystem crossing process of a non-emissive triplet state (note that a detailed photophysical study will be published elsewhere). When moving to solid state, the photophysics of the compounds are governed by the present intermolecular

This journal is © The Royal Society of Chemistry 20xx

Please do not adjust margins

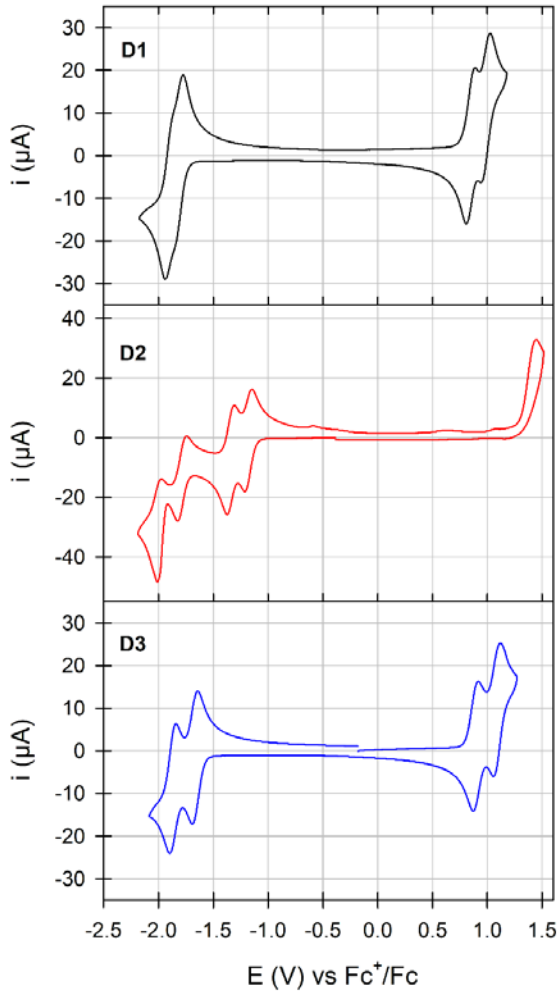


Figure 4. *Cyclic voltammogram of* ***D1*** *(top),* ***D2*** *(middle) and* ***D3*** *(bottom).*

interactions. For instance, the emission of **BTXI** is red shifted and completely quenched due to aggregation quenching as a result of the formation of the strong π-stacking intermolecular interactions described above (Figure S20). This observation is also valid for dimer **D1** with only a 0.06 quantum yield. **D2** shows a larger quantum yield of 0.14 that can be explained by the distortion induced by the sulphur oxidation reducing the π-stacking intermolecular interactions. Finally, **D3** presents a sharp emission at 580 nm strongly red-shifted (FWHM = 1442 cm^{-1} against 2348 cm^{-1} and 3145 cm^{-1} for **D1** and **D2**, respectively), accompanied by the highest quantum yield of the series. This behaviour is in agreement with the slipped π-interactions observed in the crystal structure and suggests the formation of *J*-aggregates in the solid state that are frequently observed for the perylene diimide chromophores family (Figure 3).[9]

The Cyclic voltammogram of **D1**, plotted in Figure 4, revealed the presence of two reversible and successive processes in both positive and negative regions attributed to the formation of stable cation /di-cation and anion/di-anion species respectively. While changing the grafting position (**D3**) induces a more visible splitting of the reversible processes with minor impact on their potentials (greater delocalization of charges), the conversion of the sulfurs into sulfones results in a drastic modification of the electrochemical signatures of **D2**. Indeed, on one side, the reversibility of the oxidation processes seems to be lost, while on the other side two reversible and a quasi-reversible split waves were recorded in the negative region. Thereafter, frontier molecular orbital energy levels were thus estimated from the onset of the first oxidation and reduction waves (Table 1). With almost similar LUMO levels, dimerization in the bay area (**D3** *vs* **D1**) induces a slight destabilization of the HOMO level resulting in the reduction of the gap also highlighted during the UV-visible measurements. In stark contrast, oxidation of the sulfur into sulfone causes the stabilization of both frontier orbitals while increasing the band gap. Complementarily investigated by computational chemistry, simulated frontier energy levels and UV-visible spectrum were also found to follow these experimental trends (Figure S26-28 and Table S2).

Hence, and as a further step into the characterization of these dimers and for a deeper structure-property relationship investigation, solution-processed OLED devices, of architecture: glass/ITO/PEDOT:PSS/Emitting layer (EML)/ZnO/Ag, were then fabricated.[10] The luminescent and commercially available conjugated polymer **PFO**, also known as **F8**, was used into the EMLs as a host material to improve the performances of small molecules-based OLEDs.[10, 11]

Table 2. *OLEDs performance based on PFO and/or blends with dimers.*

Emitting layer	ratio	V_{on} (V)	EQE_{max} (%)	LE_{max} (cd A^{-1})	PE_{max} (lmW^{-1})	L_{max} (cd m^{-2})
PFO:D1	2:18	4.8	0.04	0.26	0.30	608 (@9.9V)
PFO:D2	2:18	3.9	0.04	0.08	0.04	1336 (@6.9V)
PFO:D3	2:18	3.9	0.17	0.37	0.16	2860 (@ 10V)

Tested under ambient conditions, it is noteworthy that all devices emitted light when connected to an external voltage, thus demonstrating, for the first time, up and running **BTXI**-based OLEDs. An overview of the main characteristics of the three **BTXI**-based OLEDs is summarized in Table 2 and their electroluminescence spectra (EL) and the Commission Internationale de l'Eclairage (CIE) color coordinates are shown in Figure 5. In agreement with the optical properties of the three dimers, different colors of emitted lights, from blue to orange, were recorded. These results highlight, once again, the ease of

Please do not adjust margins

tunability at different levels induced by simple chemical modifications. The redshift and changing of EL shape of BTXI-based OLEDs relative to the photoluminescence is a result of the aggregation of the dimers and various formation and relaxation of exciton mechanisms in OLED structure (under voltage) and "clean" films (under light excitation).

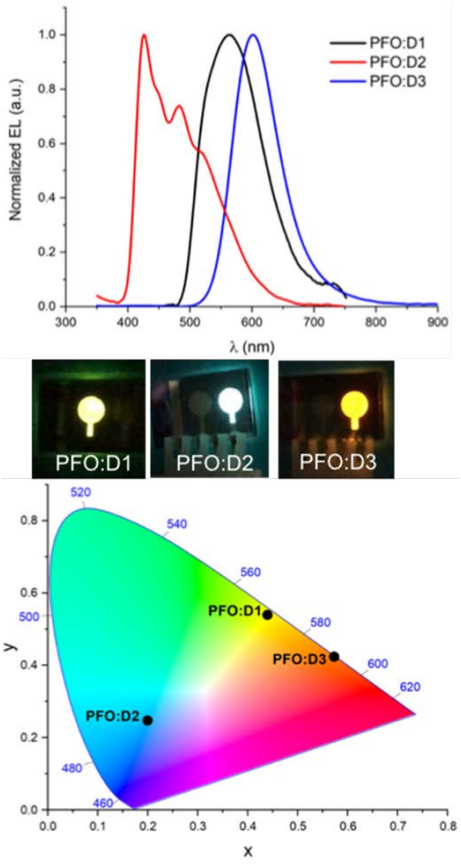


***Figure 5**. Electroluminescence spectra (top) and CIE color coordinate spectra (above) of the **D1** (black), **D2** (red) and **D3** (blue) based devices under external voltage.*

In addition, the EML layers were spin-casted from *o*-xylene which indicates that these materials can be easily transferred to develop flexible OLEDs by roll-to-roll coating into industrial scale. Moreover, the performance of these **BTXI**-based OLEDs could be improved by using a multilayer OLEDs structure.[12]

Conclusions

The synthesis and characterization of three original **BTXI**-based dimers is reported herein. Subttle chemical modifications, namely the oxidation of the constituting sulphur into sulfone and the dimerization in the bay area, were investigated as well as their impact on the optical and electrochemical properties. Due to their good solubility and highly twisted structures, these dimers were finally and successfully used as emitting materials for the demonstration of the first **BTXI**-based OLEDs.

Conflicts of interest

There are no conflicts to declare.

Acknowledgments

Authors thank the MATRIX SFR of the University of Angers. J.M.A.C. and P.S.M. thanks the European Union's Horizon 2020 research and innovation program under Marie Sklodowska Curie Grant agreement No.722651 (SEPOMO). The *Région Pays de la Loire* is also acknowledged for the grant of C. D. (Projet étoile montante SAMOA). The authors are also grateful to ANR (SADAM ANR-16-CE07-0015-01) for the financial support and PDF grant of L.A.G. S. D. thanks the MITACS program for financial support. G. C. W. thanks the University of Calgary.

Statement of Contributions

JMA: synthesis, characterization and writing of the ESI, CD: synthesis and characterization, SD: device fabrication and testing, LAG and PSM: computational chemistry, OA: electrochemical characterization, MA: crystallographic characterization, OM: LAG's PI and discussions, PB, JMA/PSM's co-PI and discussions, GW: SD's PI and discussions, CC: CD's PI and JMA/PSM's co-PI, writing of the article

Notes and references

1. T. Weil, T. Vosch, J. Hofkens, K. Peneva and K. Müllen, *Angewandte Chemie International Edition*, 2010, **49**, 9068-9093.
2. F. Würthner, C. R. Saha-Möller, B. Fimmel, S. Ogi, P. Leowanawat and D. Schmidt, *Chemical Reviews*, 2016, **116**, 962-1052.
3. P. Josse, S. Li, S. Dayneko, D. Joly, A. Labrunie, S. Dabos-Seignon, M. Allain, B. Siegler, R. Demadrille, G. C. Welch, C. Risko, P. Blanchard and C. Cabanetos, *Journal of Materials Chemistry C*, 2018, **6**, 761-766.
4. C. Dalinot, P. Simón Marqués, J. M. Andrés Castán, P. Josse, M. Allain, L. Abad Galán, C. Monnereau, O. Maury, P. Blanchard and C. Cabanetos, *European Journal of Organic Chemistry*, 2020, **2020**, 2140-2145.
5. S. V. Dayneko, A. D. Hendsbee, J. R. Cann, C. Cabanetos and G. C. Welch, *New Journal of Chemistry*, 2019, **43**, 10442-10448.
6. A.-J. Payne, N. A. Rice, S. M. McAfee, S. Li, P. Josse, C. Cabanetos, C. Risko, B. H. Lessard and G. C. Welch, *ACS Applied Energy Materials*, 2018, **1**, 4906-4916.
7. A. D. Hendsbee, J.-P. Sun, W. K. Law, H. Yan, I. G. Hill, D. M. Spasyuk and G. C. Welch, *Chemistry of Materials*, 2016, **28**, 7098-7109.
8. L. A. Galán, J. M. Andrés Castán, C. Dalinot, P. S. Marqués, P. Blanchard, O. Maury, C. Cabanetos, T. Le Bahers and C. Monnereau, *Physical Chemistry Chemical Physics*, 2020, **22**, 12373-12381.
9. S. Herbst, B. Soberats, P. Leowanawat, M. Stolte, M. Lehmann and F. Würthner, *Nature Communications*, 2018, **9**, 2646.
10. S. V. Dayneko, M. Rahmati, M. Pahlevani and G. C. Welch, *Journal of Materials Chemistry C*, 2020, **8**, 2314-2319.
11. J. H. Ahn, C. Wang, I. F. Perepichka, M. R. Bryce and M. C. Petty, *Journal of Materials Chemistry*, 2007, **17**, 2996-3001.
12. M. Rahmati, S. V. Dayneko, M. Pahlevani and G. C. Welch, *ACS Applied Electronic Materials*, 2020, **2**, 48-55.

This journal is © The Royal Society of Chemistry 20xx

Please do not adjust margins

Please do not adjust margins

This journal is © The Royal Society of Chemistry 20xx

Please do not adjust margins